

Phonon Mechanism of the Magnetostructural Phase Transition in MnAs

J. Łażewski,^{1,*} P. Piekarczyk,¹ J. Tobała,² B. Wiendlocha,² P. T. Jochym,¹ M. Sternik,¹ and K. Parlinski¹

¹*Institute of Nuclear Physics, Polish Academy of Sciences, Radzikowskiego 152, 31-342 Kraków, Poland*

²*Faculty of Physics and Nuclear Techniques, Academy of Mining and Metallurgy, Mickiewicza 30, 30-073 Kraków, Poland*

(Received 17 September 2009; published 7 April 2010)

Density functional theory was used to study structural and dynamical changes related to the magnetostructural phase transition in MnAs. The soft mode inducing the transition from the high-symmetry hexagonal to the low-symmetry orthorhombic phase was revealed. A giant coupling between the soft mode and magnetic moments was found and its crucial role in the magnetostructural transition was established. The estimated phonon contribution to the total entropy change has the opposite sign to the magnetic entropy change.

DOI: [10.1103/PhysRevLett.104.147205](https://doi.org/10.1103/PhysRevLett.104.147205)

PACS numbers: 75.30.Sg, 31.15.es, 63.20.dk

In recent years a well-known transition metal compound MnAs has attracted renewed attention, due to a giant magnetocaloric effect (MCE) reported by Wada and Tanabe [1]. Notably, MnAs shows the MCE properties comparable to those of the rare-earth compound $\text{Gd}_5(\text{Si}_2\text{Ge}_2)$, in which the giant MCE was for the first time described by Pecharsky and Gschneider [2]. Under ambient pressure the maximum entropy change in MnAs can achieve $\Delta S = S_\alpha - S_\beta = -30 \text{ J}/(\text{K kg})$ [1,3] for magnetic field change $\Delta H = 5 \text{ T}$ and $-20 \text{ J}/(\text{K kg})$ for $\Delta H = 2 \text{ T}$ [4]. Such remarkable solid state behavior may enable magnetic refrigeration applications at room temperature. The idea is based on the magnetocaloric phenomenon related to reversible processes of heating up and cooling down magnetic materials by inserting into and withdrawing from an external magnetic field repeatedly in adiabatic conditions. In fact, MnAs is one of the most promising magnetic materials for refrigeration near ambient temperature, due to a strong magnetostructural transition occurring at $T_c \sim 315 \text{ K}$, resulting from a particular interplay between magnetic and lattice degrees of freedom.

The hexagonal ferromagnetic (FM) α -MnAs (NiAs-type, $P6_3/mmc$) undergoes a first-order phase transition to the orthorhombic paramagnetic (PM) β -MnAs (MnP-type, $Pnma$) phase at T_c [5]. The first-order magnetic phase transition ($\alpha \rightarrow \beta$) is accompanied by a large volume contraction ($\sim 2\%$), related to the hexagonal-orthorhombic structural transition. At higher temperature $T_t \sim 393 \text{ K}$, the compound returns to the hexagonal NiAs-type structure (γ -MnAs) with $P6_3/mmc$ space group, through a second-order phase transition, maintaining, however, a PM state.

A complex phase diagram of MnAs indicates quite unique coupling between magnetism and the crystal structure. The first phenomenological model, proposed by Bean and Rodbell [6], assumed explicit dependence of the critical temperature T_c on volume. This model successfully explains the first-order character of the $\alpha \rightarrow \beta$ phase transition. The phase diagram was derived from a more ad-

vanced model, with two competing order parameters, magnetization and lattice distortion, developed within the Landau theory by Pytlík and Zieba [7]. Earlier, on the basis of the electron band structure, Goodenough and Kafalas [8] had proposed the mechanism combining the lattice deformation with transition from the high-spin to the low-spin state. The low-spin state ($S = 0$), however, has not been detected in the neutron scattering experiment [9], and the microscopic origin of the strong magnetoelastic coupling still needs further studies.

The crystal structure and FM moments in the α phase, obtained by density functional theory (DFT), agree very well with the experimental data [10]. However, a magnetic arrangement in the PM orthorhombic phase has not yet been fully understood. The effect of the orthorhombic distortion on the magnetic ground state was studied by mapping of the DFT total energy onto the Heisenberg model [11]. It has been found that for the critical distortion, the FM state changes into the antiferromagnetic (AFM) state. A similar result has been obtained for the β phase, studied as a function of magnetic ordering [12]. Although the AFM state has not been observed in the orthorhombic phase, these studies demonstrate a strong coupling between the crystal structure and magnetic interactions in MnAs.

The lattice dynamics in MnAs have not been investigated so far, but some measurements, including the elastic modulus and sound attenuation, indicate that phonons participate in the $\alpha \rightarrow \beta$ phase transition [13]. The anomalous behavior of the Debye-Waller factor close to the phase transition at T_c suggests the critical lowering of phonon frequencies [14]. A soft-mode mechanism of the structural transition has been suggested as consistent with the observed magnetic origin of the entropy change [3].

In this Letter, we present, for the first time, the phonon dispersion relations obtained for the α phase. We study the changes of the phonon spectrum induced by magnetic interactions and external pressure invoking volume changes. We focus on a giant spin-phonon coupling, which drives the first-order magnetostructural transition in MnAs.

To our best knowledge, such strong magnetic-phonon interaction is unique, and has not been observed in other materials.

We have performed first-principles calculations based on the spin-polarized DFT as implemented in the VASP package [15]. In present calculations, the Blöchl full potential projector augmented-wave method [16], within the generalized gradient approximation [17], has been employed. The Brillouin-zone integration has been carried out with a $4 \times 4 \times 4$ k -point mesh generated with the Monkhorst-Pack scheme [18]. The plane-wave basis set was limited by a kinetic energy cutoff at 320 eV. For structural and phonon calculations we have used the $2 \times 2 \times 1$ supercell containing 16 atoms. As a standard procedure we checked the convergence of calculations with kinetic energy cutoff and the density of k -point mesh. In addition, a larger supercell with 72 atoms has been used for checking the convergence of the lattice parameters and phonon frequencies with the supercell size. Phonon dispersion relations have been calculated using the direct method [19] as implemented in the PHONON program [20]. The force constants and dynamical matrix have been obtained from the Hellmann-Feynman forces calculated with small individual displacements of nonequivalent atoms.

The crystal structure of MnAs has been optimized assuming the FM ordering on Mn atoms. For the hexagonal structure, we have obtained the lattice parameters $a = 3.666 \text{ \AA}$ and $c = 5.508 \text{ \AA}$ in close agreement with the experimental data taken at $T = 110 \text{ K}$: $a_{\text{expt}} = 3.733 \text{ \AA}$ and $c_{\text{expt}} = 5.677 \text{ \AA}$. Comparing to the experimental magnetic moment on Mn atoms ($3.4 \mu_B$), we have obtained a smaller value $3.05 \mu_B$ for optimized hexagonal structure. However, for the experimental values of lattice constants we have found $3.35 \mu_B$. The optimization in the orthorhombic supercell with the FM ordering of magnetic moments leads to a very similar structure, which has atomic positions different by 0.01 \AA at the most. The difference of total energies between both structures is less than 0.6 meV per atom. The calculations were repeated for a wide range of pressures from -50 to 20 kb , where negative pressures (larger volume) correspond to higher temperatures.

The calculated phonon dispersion relations for the hexagonal phase along the high-symmetry directions are plotted in Fig. 1. At $p = 0$, all phonon energies are positive, which ensures the dynamical stability of the hexagonal phase in ambient conditions. There is, however, a low-energy phonon at the M point, whose frequency strongly depends on pressure. For positive pressures, the energy of the soft mode rapidly decreases and goes to zero around $p = 25 \text{ kb}$. Consequently, negative pressure increases the frequency of the soft mode. This soft mode is responsible for the structural transition between the hexagonal and orthorhombic phases. The calculated critical pressure for the $\alpha \rightarrow \beta$ transition cannot be compared with the experimental value at low temperature ($\sim 3.6 \text{ kb}$), since the

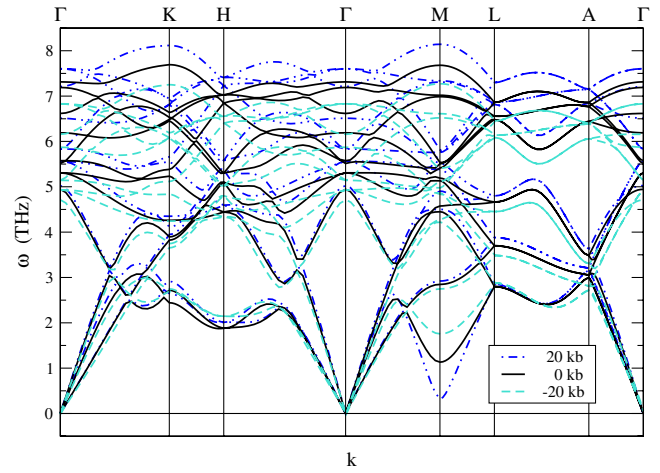


FIG. 1 (color online). Phonon dispersion relations for hexagonal phase calculated under several pressures. For values of optimized volume and soft-mode frequencies, see Table I.

theoretical value was obtained assuming the continuous change of volume with the unchanged FM order. In fact, crystal volume collapses due to the magnetic transition and—in consequence of the coupling with the soft mode—it leads to the first-order phase transition with a lower critical pressure. The soft-mode frequencies, magnetic moments, and crystal volumes for all pressures used in the calculations are presented in Table I.

A symmetry analysis based on the Stokes and Hatch tables [21] shows that the soft mode observed in the hexagonal structure reduces crystal symmetry to the orthorhombic space group ($Pnma$) according to the diagram

$$P6_3/mmc \rightarrow [M_2^+, \mathbf{k} = (0.5, 0, 0)] \rightarrow Pnma. \quad (1)$$

A change of the Mn-Mn distance induced by the soft mode originates from a giant spin-phonon coupling present in MnAs. To study this coupling, we have calculated dispersion curves as a function of the magnetic moment on Mn. For the nonmagnetic state ($m = 0$), the phonon spectra obtained for both phases show many imaginary modes which make the crystal unstable. This demonstrates that magnetic interactions are crucial to stabilize the crystal lattice of MnAs. The above finding also applies to the PM state, where the crystal structure is stabilized by the fluctuating magnetic moments.

TABLE I. Volume, magnetic moment, and soft-mode frequency versus pressure, calculated for MnAs hexagonal phase.

p (kb)	V (\AA^3)	$\Delta V/V_0$	ω_{soft} (THz)	m (μ_B)
-50	282.04	1.099	2.280	3.47
-20	266.71	1.040	1.756	3.24
-10	260.53	1.016	1.333	3.12
0	256.52	1.000	1.133	3.05
10	253.15	0.987	0.760	2.99
20	249.85	0.974	0.322	2.93

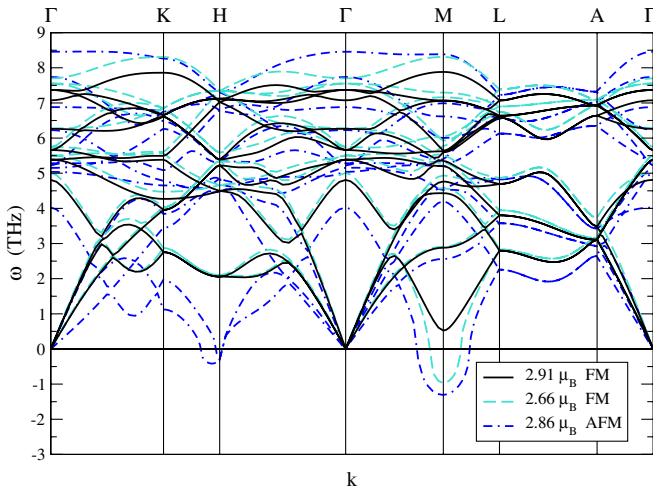


FIG. 2 (color online). Phonon spectra in the hexagonal phase calculated with fully relaxed 16-atoms supercell for a few fixed values of magnetic moment on Mn atoms at 0 kb pressure.

The phonon dispersion curves in the α phase, plotted for different values and ordering of the magnetic moment, are shown in Fig. 2. Dramatically reduced magnitudes of m (far below experimental values) have been selected intentionally to underline the strength of the spin-phonon coupling. For the reduced moment, the same mode at the M point softens and goes to zero around $m \sim 2.8\mu_B$. This unusual result demonstrates a very strong coupling between the soft phonon mode and magnetization. Because of this coupling the increased magnetic moment stabilizes the hexagonal phase, while the decreased moment induces the orthorhombic distortion. In a first-order phase transition, the phonon softening is not complete, so such a strong decrease of magnetic moments has not been observed. To estimate the strength of the spin-phonon coupling λ , we have fitted dependence of the soft-mode frequency on spin correlations to the formula

$$\omega = \omega_0 + \lambda \langle \mathbf{S}_i \cdot \mathbf{S}_j \rangle, \quad (2)$$

implemented previously to spinels [22]. Assuming for the FM configuration $\langle \mathbf{S}_i \cdot \mathbf{S}_j \rangle = S^2 = \frac{1}{4}m^2$, we have obtained $\lambda = 4.04$ THz, which is much larger than values reported for strongly frustrated magnets [23]. It confirms the extremely strong character of this coupling. Fitted ω_0 has the negative sign and well corresponds to the value of soft-mode frequency calculated for the nonmagnetic system.

Lowering of the magnetic moment and phonon softening are associated with shortening of the Mn–Mn distance and decrease of volume, as observed in the $\alpha \rightarrow \beta$ transition. It appears that the coupling between magnetization and crystal volume, due to the soft-mode driven structure transformation, plays a key role in the magnetostructural transition of MnAs. Additionally, a strong dependence of the structural stability on the Mn magnetic moment explains, in a similar way, the effect of the external magnetic field on the phase transition (i.e., shift of T_c towards higher temperature).

The scheme of atom displacements obtained from the polarization vector of the soft mode is presented in the inset of Fig. 3. Mn atoms move primarily in the hexagonal a - b plane in one direction, while As atoms move along the c direction. These atomic displacements are consistent with the orthorhombic distortion observed in the diffraction measurements [5]. Moreover, the increase of Mn atoms displacement (u_{Mn}), corresponding to the β phase stabilization, reduces the value of m (see Fig. 3). It suggests that in the disordered PM state m is about 10% smaller than in the ordered FM one. Under pressure, the dependence of the total energy on u_{Mn} shows flattening, characteristic for the system destabilization. Indeed, for $p = 20$ kb the hexagonal phase is close to the transition point and the soft-mode frequency is only 0.322 THz (see Table I). At this pressure, the magnetic moment shows even stronger dependence on the soft-mode amplitude, indicating a larger spin-phonon coupling close to the phase transition. Average thermal displacements of Mn atoms, calculated from the whole phonon spectrum at T_c , are about 0.1 Å. However, taking flatness of the potential into account, vibration amplitude of the soft mode can be several times higher.

An interesting question arises: What is the influence of the local moment ordering on phonons? To investigate it, we have repeated calculations for two AFM configurations: with the in-plane and interplane staggered spin orientations. For $p = 0$ and $p = 20$ kb, we have observed volume contraction and about 7% local magnetic moment reduction. In the case of the in-plane AFM order, the spin-phonon coupling [see Eq. (2)] leads to instability at the M point with the soft-mode frequency about -1.5 THz at $p = 0$ (see Fig. 2). This confirms that magnetic disordering destabilizes hexagonal structure and through the soft mode induces the first-order phase transition to the orthorhombic phase.

As discussed previously [3], a large entropy change in the magnetostructural transition is mainly associated with

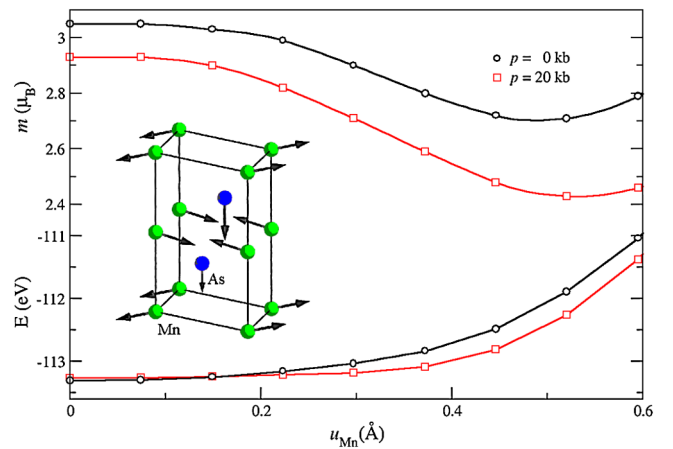


FIG. 3 (color online). The Mn magnetic moment and the total energy of the 16-atoms supercell as a function of the Mn atoms displacement in the soft mode at the M point of the Brillouin zone of hexagonal phase.

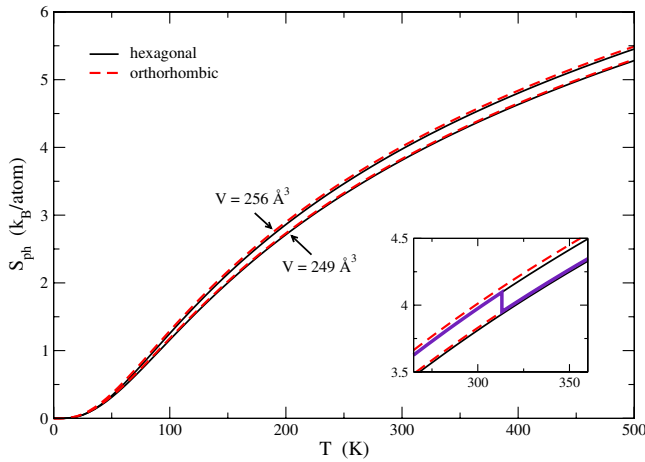


FIG. 4 (color online). Calculated phonon entropy for the hexagonal and orthorhombic structures calculated at $p = 0$ (upper curve) and $p = 20$ kb (lower curve). In the inset, we plot the change of phonon entropy at T_c .

the magnetization change. Recently, it was suggested that phonons can significantly contribute to the entropy change [24]. Here, we estimate the change in entropy associated with phonons [25]. In Fig. 4 we present comparison of the phonon entropy calculated for the hexagonal as well as orthorhombic phases for two pressures. One pressure corresponds to the high-volume hexagonal phase ($p = 0$) and the other to the low-volume orthorhombic phase ($p = 20$ kb). The relative change of the volume $\Delta V/V_0 = 0.974$ (see Table I) is consistent with the experimental value ($\sim 2\%$). For both pressures, the hexagonal phase has slightly lower values of entropy in the whole temperature range. However, differences between both phases are almost negligible. The phonon contribution to the entropy change at the phase transition can be estimated by calculating the difference in entropy obtained for these two volumes $\Delta S = S_\alpha - S_\beta$. It reads $0.146k_B/\text{atom} = 9.31 \text{ J}/(\text{kg K})$. Comparing to the experimental entropy change [3], the phonon part is much smaller and has the opposite sign. In this estimation, we take into account only the entropy change related to the volume decrease at T_c , so the influence of magnetization on phonons is only partially included.

In conclusion, a stable structure of the hexagonal phase of MnAs, with the lattice parameters and Mn magnetic moment comparable with the experimental data, was described with the first-principles calculations. A soft mode at the M point, reducing the hexagonal symmetry to the orthorhombic one, was found. We have revealed that the soft-mode frequency strongly decreases with lowering of the Mn magnetic moment. A remarkable decrease of m with the increased soft-mode amplitude appears to be the principal reason for stability loss of the hexagonal structure. Thus, this giant spin-phonon coupling plays a crucial

role in the mechanism of the $\alpha \rightarrow \beta$ phase transition in MnAs.

This work was partially supported by the European Community under COST Action P19 and by the Polish government (MNiSW) within Contract No. 44/N-COST/2007/0.

*Jan.Lazewski@ifj.edu.pl

- [1] H. Wada and Y. Tanabe, *Appl. Phys. Lett.* **79**, 3302 (2001).
- [2] V. K. Pecharsky and K. A. Gschneider, *Phys. Rev. Lett.* **78**, 4494 (1997).
- [3] J. D. Zou *et al.*, *Europhys. Lett.* **81**, 47002 (2008).
- [4] D. Fruchart *et al.*, *Physica (Amsterdam)* **A358**, 123 (2005).
- [5] R. H. Wilson and J. S. Kasper, *Acta Crystallogr.* **17**, 95 (1964).
- [6] C. P. Bean and D. S. Rodbell, *Phys. Rev.* **126**, 104 (1962).
- [7] L. Pytlík and A. Zieba, *J. Magn. Magn. Mater.* **51**, 199 (1985).
- [8] J. B. Goodenough and J. A. Kafalas, *Phys. Rev.* **157**, 389 (1967).
- [9] L. H. Schwartz, E. L. Hall, and G. P. Felcher, *J. Appl. Phys.* **42**, 1621 (1971).
- [10] P. Ravindran *et al.*, *Phys. Rev. B* **59**, 15680 (1999); S. Sanvito and N. A. Hill, *Phys. Rev. B* **62**, 15553 (2000); A. Continenza *et al.*, *Phys. Rev. B* **64**, 085204 (2001).
- [11] I. Rungger and S. Sanvito, *Phys. Rev. B* **74**, 024429 (2006).
- [12] M. K. Niranjan, B. R. Sahu, and L. Kleinman, *Phys. Rev. B* **70**, 180406(R) (2004).
- [13] K. Barner and H. Berg, *Phys. Status Solidi A* **49**, 545 (1978); J. Ihlemann and K. Barner, *J. Magn. Magn. Mater.* **46**, 40 (1984).
- [14] O. Palumbo, C. Castellano, A. Paolone, and R. Cantelli, *J. Phys. Condens. Matter* **17**, 1537 (2005).
- [15] G. Kresse and J. Furthmüller, *Comput. Mater. Sci.* **6**, 15 (1996); *Phys. Rev. B* **54**, 11169 (1996).
- [16] P. E. Blöchl, *Phys. Rev. B* **50**, 17953 (1994); G. Kresse and J. Joubert, *ibid.* **59**, 1758 (1999).
- [17] J. P. Perdew, K. Burke, and M. Ernzerhof, *Phys. Rev. Lett.* **77**, 3865 (1996).
- [18] H. J. Monkhorst and J. D. Pack, *Phys. Rev. B* **13**, 5188 (1976).
- [19] K. Parlinski, Z. Q. Li, and Y. Kawazoe, *Phys. Rev. Lett.* **78**, 4063 (1997).
- [20] K. Parlinski, software PHONON, 2008, <http://wolf.ifj.edu.pl/phonon/>
- [21] H. T. Stokes and D. M. Hatch, *Isotropy Subgroups of the 230 Crystallographic Space Groups* (World Scientific, Singapore, 1988).
- [22] A. B. Sushkov *et al.*, *Phys. Rev. Lett.* **94**, 137202 (2005).
- [23] K. T. Chan *et al.*, *Phys. Rev. B* **75**, 054304 (2007).
- [24] S. Gama *et al.*, *Phys. Rev. Lett.* **93**, 237202 (2004).
- [25] M. Born and K. Huang, *Dynamical Theory of Crystal Lattices* (Clarendon, Oxford, 1954).